

SLAC-PUB-16879

FACETII-TN-002

November 2016

Longitudinal Stability Study for the FACET-II e^+ Damping Ring ^a

Karl Bane

SLAC National Accelerator Laboratory, Menlo Park, CA 94025

^a Work supported by the U.S. Department of Energy under Contract No. DE-AC02-76SF00515

INTRODUCTION

The FACET-II e^+ damping ring is a small ring meant to reduce the emittances of the positron beam after the positron source. The details of the ring vacuum chamber have not yet been set. Nevertheless, we already know (see below) that shielded coherent synchrotron radiation (CSR) is a dominant impedance source. We will obtain a rudimentary ring impedance by adding to CSR the RF cavity impedance and necessary pipe transition impedances. But since these contributions are quite small compared to that of CSR, it will be difficult to accurately estimate their impact on the microwave threshold. At this stage we will aim to find the threshold approximately. In the future, when all the important vacuum chamber components are accounted for, we hope to find that at the nominal charge of $Q = 1$ nC the beam is either below, or at most slightly above, the threshold to the microwave instability.

Below we obtain a beginning impedance budget, generate pseudo-Green function wakes, and perform longitudinal phase space simulations. In our simulations, to make the problem manageable, we artificially reduce the damping time to $\tau_z = 200T_s$, and simulate for different values of bunch charge Q . This is followed by changing the damping time by a factor of 2 and of 3 to verify that, locally, the results are insensitive to τ_z . But in reality the damping time is much larger, with $\tau_z = 17,700T_s$. It should be verified in the future that a different phenomenon does not manifest itself in the case of such weak damping.

IMPEDANCE BUDGET

To estimate the microwave threshold for the Facet-II e^+ ring we begin by generating an impedance budget. Having as yet no engineering drawings of the vacuum chamber we consider only: the two 2-cell RF cavities, four pairs of transitions, the kicker chambers, the wall resistance, and the effect shielded coherent synchrotron radiation (CSR). Other objects that may be important and can be added in the future are the button beam position monitors (BPMs), the shielded bellows, the septa, etc. In general, the beam pipes of the ring are round. Fig. 1 gives a simplified sketch of the layout of the ring showing the relative beam pipe sizes and the locations of the two RF cavities and the two kickers. The beam pipes are round with radius $a = 0.75, 2.0, 4.0$ cm in the RF cavity and kicker sections, in the

arcs, and in the straight sections, respectively. The large aperture in the straight sections is needed to accept the injected beam with its large emittance.

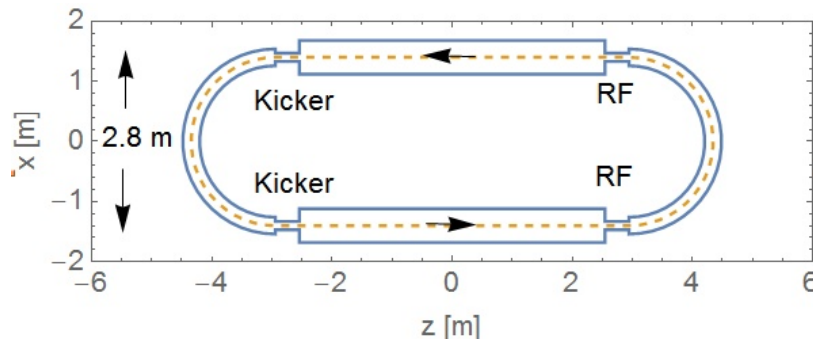


FIG. 1. Simplified sketch of the layout of the FACET e^+ damping ring used in this study, showing the relative size of the beam pipes in the different regions. The beam pipes are round with radius $a = 0.75, 2.0, 4.0$ cm in the RF cavity and kicker sections, in the arcs, and in the straight sections, respectively. The locations of the cavities and kickers are also indicated. The arrows give the beam's direction of motion.

RF Cavities

The RF cavities are the two 2-cell, 714 MHz cavities that were used in the SLC damping rings (see Fig. 2). They are cylindrically symmetric, and one cavity will be located in each straight section of the FACET ring. The external beam pipes, as well as the minimum aperture, have a radius of 7.5 mm. To obtain the wakefield, we use I. Zagorodnov's ECHO program [1], using as driving bunch a Gaussian with rms length $\sigma_z = 3.5$ mm (the nominal bunch after it has been lengthened by IBS). The bunch wake $W_\lambda(s)$ of the two 2-cell cavities in the ring is shown in Fig. 3 (the blue curve); the bunch shape $\lambda(s)$ is also shown, with the head to the left (black dots).

The wake of the RF cavities for the SLC damping rings has been approximated with a resistive model [2]; *i.e.* one given by a bunch wake of the form

$$W_R(s) = -cR\lambda(s) , \quad (1)$$

with c the speed of light and R the resistance, a constant. From Fig. 3 we see that the resistive model is a good approximation to the cavity bunch wake (*i.e.* the shape of the

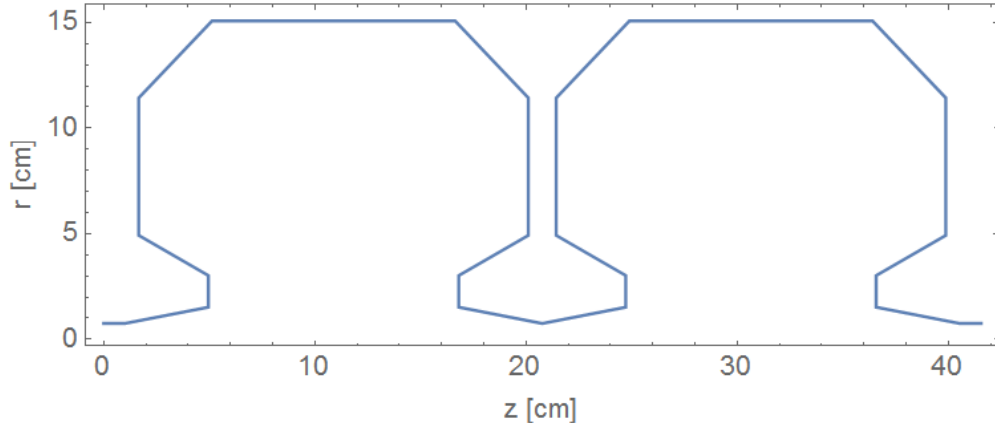


FIG. 2. The shape of one 2-cell SLC damping ring RF cavity. The beam pipe radius, as well as the minimum aperture, is 7.5 mm.

cavity wake is similar to $-\lambda(s)$. Fitting the bunch wake to the model (and weighting by the Gaussian distribution) we find an effective (per cavity) resistance, $R = 193 \Omega$.

Transitions

The beam pipe in the ring is mostly round, with radius $a = 2$ cm in the arcs, $a = 4$ cm in the straights, and $a = 0.75$ cm in the RF cavity and kicker sections (see Fig. 1). We see that at least 8 (round) beam pipe transitions are needed in the ring, four connecting $a = 0.75$ cm to 2 cm, and four connecting $a = 0.75$ cm to 4 cm. Let us first consider non-tapered step transitions. If $\sigma_z/a_1 \ll 1$, where a_1 is the smaller of the two beam pipes (which is approximately satisfied here, where $\sigma_z = 3.5$ mm and $a_1 = 7.5$ mm), we can use the optical model to approximate the wake of the step transitions. According to this model, the wake of a symmetric pair of step transitions (between radius a_1 and a_2 with $a_2 > a_1$) is resistive with resistance given by [3]

$$R = \frac{Z_0}{\pi} \ln \left(\frac{a_2}{a_1} \right) \quad (a_2 > a_1), \quad (2)$$

with $Z_0 = 377 \Omega$. If we add the effect of all 8 transitions (four transition pairs), we find that $R_{tot} \approx 637 \Omega$. Thus, the beam pipe transitions in the FACET ring—if not tapered—have the same type of impedance, but a factor 1.6 times stronger, than the two RF cavities.

We can reduce the strength of the impedance of the transitions by tapering them. However, we cannot taper them too much, since we are limited in how much of the ring circumfer-

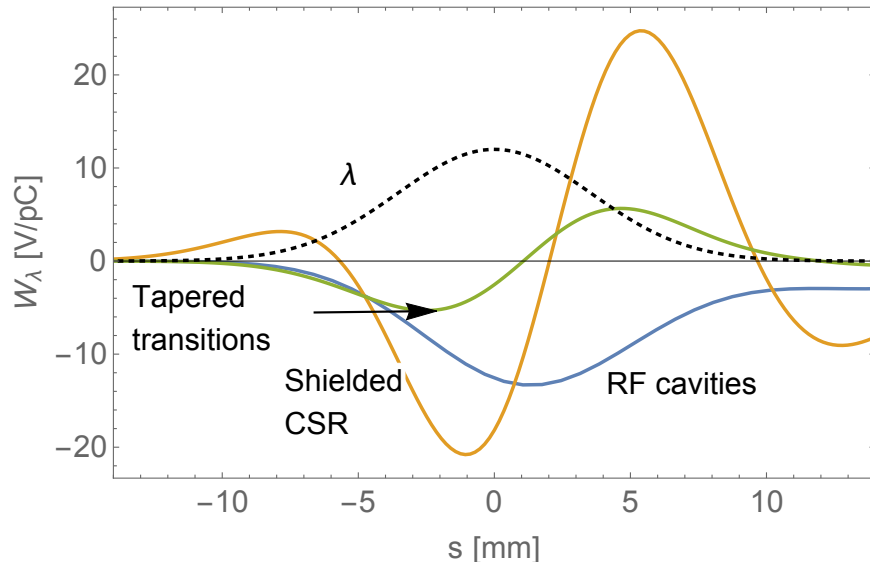


FIG. 3. The bunch wake for a Gaussian bunch with $\sigma_z = 3.5$ mm due to: two 2-cell RF cavities (blue curve), the shielded CSR in the ring (red), and the 8 tapered transitions (green). The bunch distribution $\lambda(s)$, with the head to the left, is also shown (black dots).

ence is available for this purpose. When transitions are sufficiently tapered, their impedance becomes primarily inductive, and the more the taper, the smaller the impedance becomes. We choose to taper the transitions with taper angle $\theta = 10^\circ$. With the 8 transitions, this means that the tapers—in total—will take up 1.0 m of the ring circumference.

For a symmetric pair of tapered transitions connecting beam pipes of radii a_1 and a_2 ($a_2 > a_1$) at a small angle θ , the impedance is approximately inductive, $Z(\omega) = i\omega\mathcal{L}$, with \mathcal{L} the inductance, where [4]

$$\mathcal{L} = \frac{Z_0}{2\pi c}(a_2 - a_1) \tan \theta \quad (a_1 \tan \theta \ll c/\omega, a_2 > a_1). \quad (3)$$

For this estimate to be valid requires that, for our Gaussian bunch, $\sigma_z \gg a_1 \tan \theta$ (for $a_1 = 0.75$ cm, this means that $\theta \ll 25^\circ$). Note that an important parameter in instability theory is $|\bar{Z}/n|$, with \bar{Z} the impedance at a representative frequency, and $n = \omega/\omega_0$, where ω is frequency and $\omega_0 = 2\pi c/C$, with C the ring circumference. For an inductive impedance $|\bar{Z}/n| = \omega_0\mathcal{L}$.

We have performed ECHO calculations for the nominal Gaussian bunch, for a pair of

both types of transitions. The sum of the wakes representing all 8 transitions is given by the green curve in Fig. 3. We have assumed that the transitions are not close to one another or close to the cavities (we assume their spacing is at least several times the larger pipe radius). We see that the total wake is smaller in amplitude than that of the RF cavities (blue curve), and that the character is markedly inductive—*i.e.* the shape is similar to $-\lambda(s)'$. We fit the wakes to the sum of a purely resistive wake plus a purely inductive wake:

$$W_{R+L}(s) = -cR\lambda(s) - c^2\mathcal{L}\lambda'(s) . \quad (4)$$

Per transition we find that the fitted $R = 3.3 \Omega$ and $\mathcal{L} = 0.22$ nH for the 0.75–2 cm transitions, and $R = 10.6 \Omega$ and $\mathcal{L} = 0.05$ nH for the 0.75–4 cm transitions. We define a goodness-of-fit parameter by

$$g_{fit} = 1 - \sqrt{\int [W_\lambda(s) - W_{R+L}(s)]^2 \lambda(s) ds} / \sqrt{\int W_\lambda^2(s) \lambda(s) ds} . \quad (5)$$

For both of the transitions we find that the model fits well, and that $g_{fit} = 0.74$.

We can approximate $|\bar{Z}/n|$ from the model fit using

$$\frac{\bar{Z}}{n} = \frac{\omega_0 \sigma_z}{c} R + i\omega_0 \mathcal{L} . \quad (6)$$

We find that for the four 0.75–2 cm transitions, $|\bar{Z}/n| = 0.04 \Omega$; for the four 0.75–4 cm transitions, $|\bar{Z}/n| = 0.18 \Omega$.

Shielded CSR Wake

When the FACET bunch moves through the arcs of the ring it will radiate energy coherently, and the effect on the beam can be described by the parallel plate model of coherent synchrotron radiation (CSR) [5]. The model considers the CSR wakefield generated by an electron moving on a circular orbit with bending radius ρ in the middle of two parallel plates separated by distance $2h$. This steady-state formula is applicable when the so-called formation length, $\ell_f = 4a^2/(\pi^2\sigma_z)$, is small compared to the magnet lengths [6]. Taking $a = 2$ cm, $\sigma_z = 3.5$ mm, we find that $\ell_f = 5$ cm, which is indeed small compared to the magnet lengths; thus the steady-state formula for CSR does apply.

In the case of no shielding the wake is non-zero only for negative s , (*i.e.* with the test particle ahead of the driving charge). The point charge wake is given by

$$W_{\delta 0}(s) = -\frac{Z_0 c}{3^{4/3}} H(-s) \frac{\rho^{1/3}}{(-s)^{4/3}}, \quad (7)$$

with $H(s) = 1$ for $s \geq 0$, $H(s) = 0$ for $s < 0$. With shielding, the wake $W_{\delta}(s) = W_{\delta 0}(s) + W_{\delta 1}(s)$, with

$$W_{\delta 1}(s) = -\left(\frac{Z_0 c}{4\pi}\right) \rho^{1/3} \left(\frac{\Pi}{\sigma_{z0}}\right)^{4/3} G\left(-\frac{\Pi s}{\sigma_{z0}}\right), \quad (8)$$

where the shielding parameter $\Pi = \sigma_{z0} \rho^{1/2} / h^{3/2}$, and σ_{z0} is the nominal bunch length. The term $W_{\delta 1}(s)$ is in general non-zero for both signs of argument. The function $G(\zeta)$ is given by

$$G(\zeta) = 8\pi \sum_{k=1}^{\infty} \frac{(-1)^{k+1} Y_k(\zeta) [3 - Y_k(\zeta)]}{k^2 [1 + Y_k(\zeta)]^3}, \quad (9)$$

where Y_k is a root of the equation

$$Y_k - \frac{3\zeta}{k^{3/2}} Y_k^{1/4} - 3 = 0. \quad (10)$$

This equation has two real, positive roots and two complex roots. We choose the smaller real root when $\zeta < 0$, the larger real root when $\zeta > 0$. Normally we sum k up to 25.

To find the bunch wake we convolve the two pieces of the point charge wake with the bunch distribution (the first piece is handled specially), and then add the results. In detail, we find

$$W_{\lambda 0}(s) = -\frac{Z_0 c}{3^{1/3}} \rho^{1/3} \int_0^s \frac{\lambda'(s-s')}{(s')^{1/3}} ds', \quad W_{\lambda 1}(s) = \int_{-\infty}^{\infty} W_{\delta 1}(s') \lambda(s-s') ds', \quad (11)$$

where $\lambda'(s) \equiv d\lambda(s)/ds$.

In the FACET damping ring the beam pipe in the arcs is round, with radius $a = 2$ cm. We take this to be the half-gap between the two plates of the model, *i.e.* we let $h = 2$ cm. In addition, $\rho = 0.78$ m and the nominal bunch length (including IBS) $\sigma_{z0} = 3.5$ mm. The wake of a Gaussian bunch due to shielded CSR is shown by the red curve in Fig. 3. We see that the CSR wake, at the nominal bunch length, dominates over the contributions of the RF cavities and of the tapered transitions. Fitting to the model of a resistive plus inductive wake we obtain $R = 373 \Omega$ and $\mathcal{L} = 7.4$ nH, and a goodness of fit parameter, $g_{fit} = 0.43$. We see that the model does not fit well.

In Fig. 4 we give the total wake—the sum of RF cavity, transition, and CSR contributions—for the 3.5 mm Gaussian bunch (the blue curve). In addition, we plot the wake minus the CSR contribution in dashed red, and see that CSR dominates the wake.

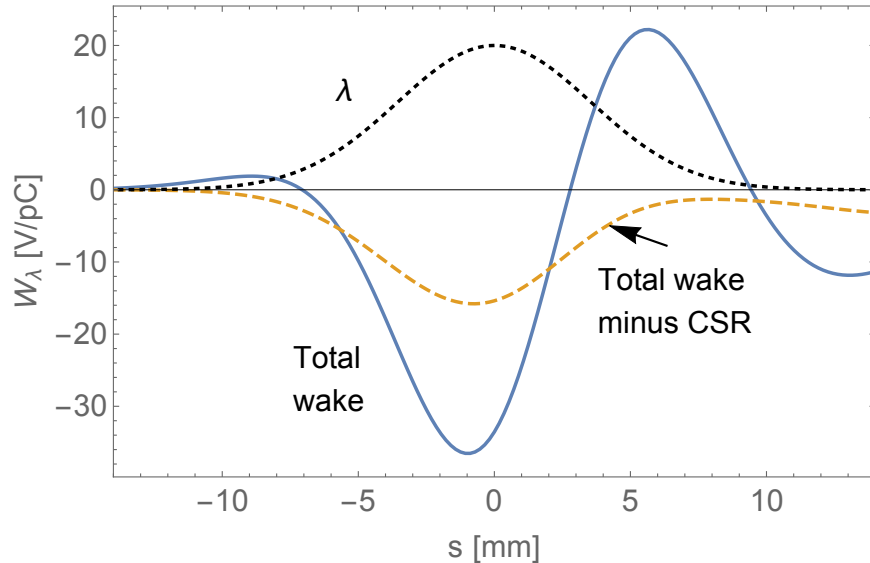


FIG. 4. The total, single turn, bunch wake for a Gaussian bunch with $\sigma_z = 3.5$ mm passing through the storage ring (assuming tapered transitions; the blue curve). The red dashed curve gives the total wake minus the shielded CSR contribution. The bunch distribution λ , with the head to the left, is also shown (black dots).

In Table I we give an impedance budget, summarizing the fitting discussed above. We also include the effect of the two kicker chambers and the wall resistance, both of which contribute a small amount of impedance compared to the three types of wake sources discussed above. In total we have resistance $R = 832 \Omega$, inductance $\mathcal{L} = 10.4$ nH, and effective impedance factor $|\bar{Z}/n| = 1.45 \Omega$. Finally, note that if we take the total wake function of Fig. 4 (the blue curve) and fit to the $R + \mathcal{L}$ model, we see that there is some cancellation: $R = 823 \Omega$, $\mathcal{L} = 8.8$ nH, and $|\bar{Z}/n| = 1.19 \Omega$. Here the goodness-of-fit parameter $g_{fit} = 0.83$.

TABLE I. Simple impedance budget for the Facet-II e⁺ damping ring. To quantify the contribution of the objects, the wake of a Gaussian bunch with $\sigma_z = 3.5$ mm, obtained by ECHO, was fit to that of the sum of a purely resistive plus inductive object, with the fit weighted by the Gaussian bunch distribution (the RF cavity wake was fit to only a resistive impedance). Column 4 gives the goodness of fit, g_{fit} . The effective $|\bar{Z}/n|$ is obtained from the fitted R and \mathcal{L} .

Object	Single Element			Total Contribution			
	R [Ω]	\mathcal{L} [nH]	g_{fit}	Number	R [Ω]	\mathcal{L} [nH]	$ \bar{Z}/n $ [Ω]
RF cavities	193.	—	0.78	2	386.	—	0.41
Tapered transitions:							
0.75–2 cm	3.3	0.22	0.74	4	13.2	0.86	0.04
0.75–4 cm	10.6	0.50	0.74	4	42.6	1.98	0.18
Kicker chambers	7.	0.04	0.57	2	14.	0.08	0.02
Resistive wall	3.5	0.05	0.84	1	3.5	0.05	0.01
Shielded CSR	373.	7.4	0.43	1	373.	7.4	0.79
Total					832.	10.4	1.45

INSTABILITY

Boussard Criterion

As a first estimate of the instability threshold, often the Boussard criterion is used. It is known to give a rough and conservative estimate of the threshold to a strong instability. According to this criterion, the threshold bunch charge is given by [7]

$$Q_{th} = (2\pi)^{3/2} \frac{\alpha \sigma_z E \sigma_\delta^2}{c |\bar{Z}/n|}, \quad (12)$$

with α the momentum compaction factor, E the beam energy, σ_δ the relative beam energy spread, and \bar{Z}/n the impedance at a representative frequency. For the FACET ring, taking $\alpha = 0.0584$, $E = 335$ MeV, $\sigma_\delta = 7.2 \times 10^{-4}$ (IBS increased value), and $|\bar{Z}/n| = 1.19 \Omega$ (the effective impedance obtained from the final wake), we obtain $Q_{th} = 1.59$ nC, which is 60% larger than the design charge.

Besides the strong instability, there is also the so-called *weak instability* [8]. It is weak in that it can be Landau damped by incoherent tune spread, and the threshold varies with the

longitudinal damping time as $Q_{th} \sim \tau_z^{-1/2}$. If the impedance is resistive, which implies it has little tune spread, then the weak instability can be excited at a lower current than the strong instability.

CSR Instability

It can be shown that for a beam in a machine dominated by the CSR impedance, the instability threshold depends only on two dimensionless parameters, the shielding parameter Π and the normalized charge $S_{\text{CSR}} = I\rho^{1/3}/\sigma_{z0}^{4/3}$, where

$$I = \left(\frac{Z_0 c}{4\pi} \right) \frac{eQ}{2\pi\nu_{s0} E_0 \sigma_{\delta 0}}, \quad (13)$$

with Q the bunch charge; with ν_{s0} , E_0 , $\sigma_{\delta 0}$, the nominal (zero current) values of synchrotron tune, energy, and relative energy spread [9]. From simulations of the Vlasov-Fokker-Planck equation, it was found that, for a ring consisting of the CSR impedance alone, the threshold to the microwave instability is well approximated by $(S_{\text{CSR}})_{\text{th}} = 0.50 + 0.12\Pi$ [9], a result that is true away from the region $\Pi \sim 0.35\text{--}1.0$. (Within this region, the weak instability appears already at a lower current, one whose exact value depends on the longitudinal damping time.) Note that for some storage rings with short bunches, such as the Metrology Light Source [10] and ANKA [11] in Germany, this simple model has been shown to agree quite well with threshold measurements.

In the FACET damping ring the beam pipe in the arcs is round, with radius $a = 2$ cm. We take this to be the half-gap between the two plates of the model, *i.e.* we let $h = 2$ cm. In addition, $\rho = 0.78$ m, $\nu_{s0} = 0.0383$, $E_0 = 335$ MeV; $\sigma_{z0} = 3.5$ mm and $\sigma_{\delta 0} = 7.3 \times 10^{-4}$ (the relative bunch length and energy spread when including the effect of IBS). Thus, the shielding parameter $\Pi = 1.11$, and the instability threshold, assuming the only impedance in the ring is the CSR impedance, is $(S_{\text{CSR}})_{\text{th}} = 0.50 + 0.12\Pi = 0.63$, which is equivalent to a threshold charge of $Q_{\text{th}} = 2.4$ nC.

Pseudo-Green Function Wake

For our instability simulations we need a wake function that we can convolve with a bunch distribution to obtain the bunch wake. For this purpose we numerically generate a wake

for a short Gaussian driving bunch that we call the *pseudo-Green function wake*, $W_\delta(s)$. The nominal bunch length is $\sigma_{z0} = 3.5$ mm. We use ECHO to obtain the wakes of the RF cavities and transitions, using a Gaussian driving bunch with $\sigma_z = 0.35$ mm, and having the calculated wakes reach to 35 mm behind the driving bunch. A similar calculation is performed analytically for the shielded CSR wake. These wakes are then summed to obtain one pseudo-Green function wake, $W_\delta(s)$, representing the entire ring. We repeat the process for the cases: (a) shielded CSR alone, (b) shielded CSR plus the rf cavities plus tapered transitions, and (c) shielded CSR plus the rf cavities plus rectangular transitions.

The pseudo-Green function wake for case (b), with the tapered transitions, is shown in Fig. 5 (the blue curve). The dashed, red curve in the figure gives the total wake minus the CSR contribution for comparison; we see that the CSR wake greatly dominates the Green function wake.

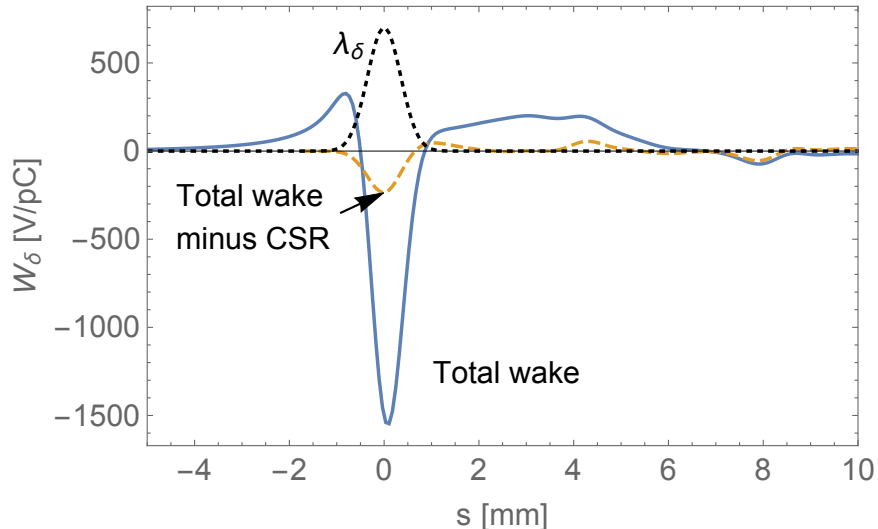


FIG. 5. The pseudo-Green function wake representing the entire ring (assuming tapered transitions; blue curve), and the wake minus the CSR contribution (red dashes). The bunch distribution $\lambda_\delta(s)$, a Gaussian with $\sigma_z = 0.35$ mm (with the head to the left), is also shown (black dots).

Simulations

To study the effect on the microwave threshold of the different impedance models we use a macro-particle tracking program (see *e.g.* [12]). For a large number M of macro-particles, the tracking program follows the energy deviation normalized to $\sigma_{\delta 0}$, p_i , and the longitudinal position normalized to σ_{z0} , q_i , over many time steps $\theta = 2\pi\Delta t/T_s$, where T_s is the synchrotron period. The equations solved are

$$\begin{pmatrix} p_i \\ q_i \end{pmatrix}_{n+1} = \begin{bmatrix} 1 - c_d & -\theta \\ (1 - c_d)\theta & 1 - \theta^2 \end{bmatrix} \begin{pmatrix} p_i \\ q_i \end{pmatrix}_n + \begin{bmatrix} 1 \\ \theta \end{bmatrix} (\theta IW_\lambda(q_i\sigma_{z0}) + r_e), \quad (14)$$

with c_d and r_e representing effects of radiation damping and quantum excitation. After each time step the particles are binned and the bunch distribution $\lambda(s)$ is recomputed. This is followed by performing convolutions like the right equation of Eq. 11, using the pseudo-Green function wake, to obtain the bunch wake.

Runs were performed for different values of charge Q , to find the charge at which the energy spread of the beam begins to increase from the nominal value. (Here the nominal energy spread and bunch length are the IBS increased values.) For the simulations, the number of macro-particles $M = 10^5$, size of domain in s is $12\sigma_z$, number of s bins is 240, time step $\Delta t = 0.02T_s$, $\tau_z/T_s = 200$. We begin with the Haissinski solution for bunch distribution, $\lambda(s)$. Calculations were performed for one or two damping times. The value of σ_δ taken as the result was the average value over several oscillations near the end of the run.

To get an idea of the accuracy of our calculations, we began the simulations by using as pseudo-Green function the shielded CSR wake alone, for a Gaussian bunch with $\sigma_z = 0.35$ mm, and varying Q in steps of 0.5 nC (case a). We obtained a rather smooth curve of σ_δ vs. Q , with the threshold at $Q_{th} \sim 1.75$ – 2.25 nC. But from the analytical fit of the (more careful) simulations of Ref. [9], discussed earlier, $Q_{th} = 2.4$ nC. Thus, believing the earlier results to be correct, we conclude that the current simulations have a slight error, one that is pessimistic. Next we repeated the calculation for case (b), shielded CSR plus RF cavities plus tapered transitions. The resulting σ_δ vs. Q curve is shown in Fig. 6. The threshold appears to be at $Q_{th} = 1.25$ nC. In Fig. 7 we give more details, showing the development of $\sigma_\delta/\sigma_{\delta 0}$ vs. t/T_s , for $Q = 1.25$ nC and 1.75 nC. We see that, after an initial damping of oscillations, the results of the former case are flat with time, whereas those of the latter

case have an increasing slope. In Fig. 6, with the red (green) plotting symbol, we show the simulation result for $Q = 1.75$ nC when the damping time was increased by a factor of 2 (3). One can see that the energy spread is not locally sensitive to damping time. Finally, we repeated the calculations for case (c), shielded CSR plus RF cavities plus rectangular transitions. The result is $Q_{th} = 1.00$ – 1.25 nC. All the simulation results are summarized in Table II.

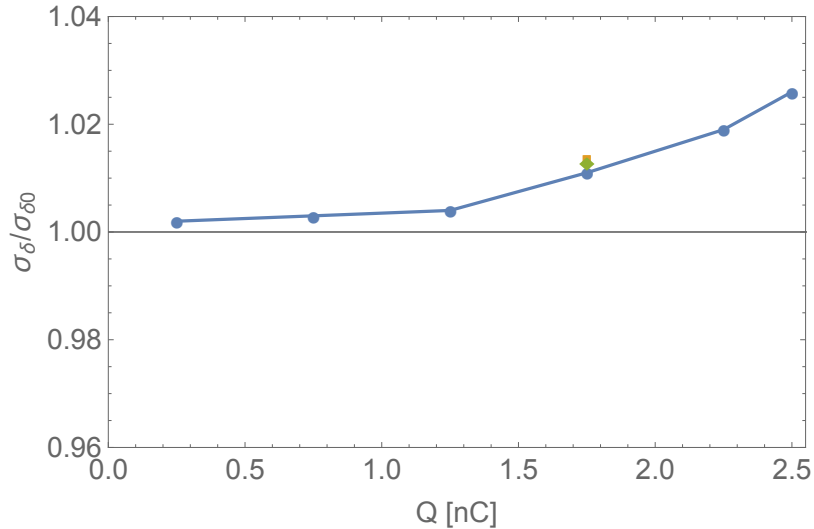


FIG. 6. Simulated energy spread after two damping times for case (b) as function of charge Q (blue). At $Q = 1.75$ nC, the case when the damping time was increased by a factor of 2 (3) is indicated by the red (green) symbol.

TABLE II. Threshold to the microwave instability in the FACET-II e^+ damping ring obtained by macro-particle simulation under various assumptions for the impedance. According to the more accurate calculations of Ref. [9] the result for (a) should be $Q_{th} = 2.4$ nC.

Case	Ring Impedance Model	Q_{th} [nC]
(a)	Shielded CSR only	1.75–2.25
(b)	Shielded CSR + RF cavities + tapered transitions	1.25
(c)	Shielded CSR + RF cavities + rectangular transitions	1.00–1.25

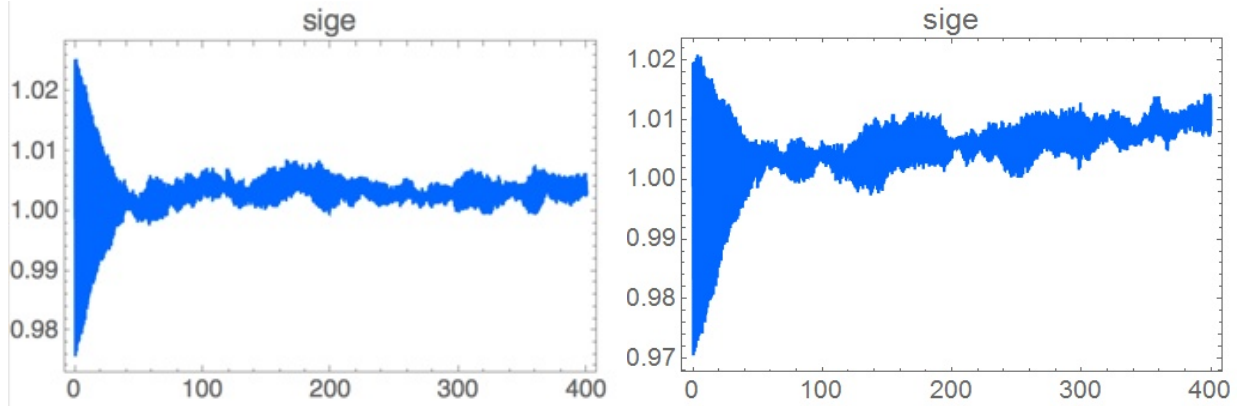


FIG. 7. For case (b), shielded CSR plus RF cavities plus tapered transitions): $\sigma_\delta/\sigma_{\delta 0}$ vs. ct/λ_s , for $Q = 1.25$ nC (left plot) and $Q = 1.75$ nC (right).

CONCLUSIONS

We have performed initial studies of the microwave instability in the FACET-II e^+ damping ring, considering a rudimentary collection of impedance objects: shielded CSR, the RF cavities, and beam pipe transitions. For the case where the transitions are tapered to angle $\theta = 10^\circ$, we find the total effective resistance, inductance, and impedance: $R = 823 \Omega$, $\mathcal{L} = 8.8$ nH, and $|\bar{Z}/n| = 1.19 \Omega$. Shielded CSR dominates the impedance.

We have performed macro-particle simulations using the pseudo-Green function approach and find that the ring is stable at the nominal charge $Q = 1$ nC with these three kinds of objects, whether the transitions are tapered or not. The fact that CSR dominates the impedance is part of the reason why it is difficult to accurately find the impact of the other objects. We have indications that the results for the threshold given here are conservative.

The simple (parallel plate) CSR model used here has worked well in predicting the bursting threshold in short bunch machines like MLS and ANKA in Germany. Nevertheless, since the CSR contribution dominates here, it might be worthwhile putting effort into CSR calculations using more realistic models—for example R. Warnock [13] and Y. Cai [14] have programs that, in principle, can calculate CSR in a square beam pipe. Also, as they become available, other impedance objects need to be included in the studies, especially objects—like the beam position monitor—that are numerous and likely significant.

In our simulations we artificially reduced the longitudinal damping time τ_z by a factor

of 100, to make the study tractable. We checked that the results were insensitive locally to changes in τ_z (to changes by a factor of 3). Nevertheless, it would still be prudent to study and verify that, with the much longer damping time of the real machine, no new physics manifests itself and invalidates the conclusions of this report.

ACKNOWLEDGMENTS

The author thanks M. Woodley and Y. Cai for helpful discussions about this ring.

REFERENCES

- [1] I.A. Zagorodnov, T. Weiland, “TE/TM field solver for particle beam simulations without numerical Cherenkov radiation,” *Phys. Rev. ST Accel. Beams* **8** (2005) 042001.
- [2] K. Bane, “The calculated longitudinal impedance of the SLC damping rings,” EPAC88, Rome, Italy, 1988, p. 637.
- [3] A. Chao et al, editors, *Handbook of Accelerator Physics and Engineering*, Second Edition, (World Scientific, New Jersey, 2013), p. 253ff.
- [4] K. Yokoya, “Impedance of slowly tapered structures,” CERN-SL-90-88-AP, July 1990.
- [5] J.B. Murphy, S. Krinsky, and R.L. Gluckstern, “Longitudinal wakefield for an electron moving on a circular orbit,” *Particle Accelerators* **57** (1997) 9.
- [6] Ya.S. Derbenev, J. Rossbach, E.L. Saldin, “Microbunch radiative tail-head interaction,” TESLA-FEL Report 1995-05, September 1995.
- [7] D. Boussard, CERN/PS-BI (1972).
- [8] K. Oide, “A mechanism of longitudinal single-bunch instability in storage rings,” KEK-Preprint-94-138, November 1994.
- [9] K. Bane, Y. Cai, and G. Stupakov, “Threshold studies of the microwave instability in electron storage rings,” *Phys. Rev. ST Accel. Beams* **13** (2010) 104402.
- [10] M. Ries et al, “THz bursting thresholds measured at the Metrology Light Source,” IPAC12, New Orleans, Louisiana, USA, 2012, p. 3030.

- [11] M. Brosi et al, "Systematic studies of short bunch-length bursting at ANKA," IPAC16, Busan, Korea, 2016, p. 1662.
- [12] P.B. Wilson, K.L. Bane, and K. Satoh, "A computer simulation of longitudinal single bunch effects in electron-positron storage rings," IEEE Trans.Nucl.Sci. **28** (1981) 2525.
- [13] R. Warnock, J. Bergstrom, and M. Klein, "Inter-bunch communication through CSR in whispering gallery modes," PAC2013, Pasadena, CA, 2013, p. 219.
- [14] Y. Cai, "Scaling law of coherent synchrotron radiation in a rectangular chamber," Phys. Rev. ST Accel. Beams **17** (2014) 020702.